Visit the
Morgan Electro Ceramics Web Site

www.morgan-electroceramics.com

Stress Sensitivity of Piezoelectric Ceramics:1 Part 3. Sensitivity to Compressive StresslPerpendicular to the Polar Axis

HELMUT H. A. KRUEGER

Measurements are reported of the change in permittivity, loss, and the piezoelectric constants, d_{31} and d_{32} for piezoelectric ceramic transducer materials subjected to high stress perpendicular to the polar axis (T1). Ceramics useful fur high-power applications PTZ-4 and PTZ-8 and some donor-doped ceramics of high .sensitivity hut with high losses that make such applications unwise (PZT-5A and PZT-5H) were tested. Permittivity generally. decreased with stress, T_1 opposite to results with parallel stress, T_3 The piezoelectric coefficient d_{31} (in the direction of stress application) decreases markedly with stress, while d_{32} (in the direction perpendicular to the stress and the polarizition) generally rises. The he effects are less severe for the "Hard" ceramics. A permanent change in pseudocrystal symmetry from ø to 2mm is observed for the donor-doped ceramics, even at relatively low stress levels (5 kpsi).

INTRODUCTION

This paper extends the study of stress sensitivity of piezoelectric ceramics to the case of static compressive stress perpendicular to the polar axis. This is referred to as lateral stress. or T_1 Properties measured are free permittivity, $\varepsilon^T_{33}/\varepsilon_{o}$, tan$\partial$ and piezoelectric coefficients d_{31} and d_{32} With no stress, $d_{31} = d_{32}$ due to the ø in pseudocrystal structure of a polarized ferroelectric ceramic. However, with stress applied laterally, d_{31} (response to incremental stress parallel to the static stress) is reduced, while d_{32} (response to incremental stress perpendicular to the static stress and perpendicular to the polar axis) generally rises. The symmetry effectively becomes 2mm. Effects on the permittivity are generally small with lateral stress, but the effects on the d constants are rather large, even for "hard" piezoelectric ceramics. For the "soft," donor-doped ceramics, permanent changes in the ratio of d_{31} to d_{32} due to exposure to lateral static stress are easily demonstrable.

For references to the general subject of stress sensitivity of transducer ceramics, the reader is referred to those listed in Part 1. However, the only works with

appreciable data on effects of one-dimensional lateral stress are by Berlincourt and Krueger' and Krueger and Berlincourt. Brown" and Nishi and Brown' have studied two. and three-dimensional effects, respectively.

Ceramics on which measurements are reported in this paper are PZT-4 and PZT-8, representative of materials suitable for high-power applications, and PZT-5A and, PZT-5H representative of materials suitable for lowpower or hydrophone purposes. These are all modified $Pb(Zr,Ti)0_3$ compositions just on the tetragonal side of the tetragonal-rhombohedral phase boundary. PZT-4 has about 5 at. % Sr^{2+} and PZT-8 has about 5% Sr^{2+} substitution for Pb^{2+} and acceptor doping (3-valent atom in B position of perovskite $AB0_3$ lattice). PZT-5A and PZT-5H have donor doping (3-valent atom in A position or 5-valent atom in B position).'

I. EXPEMMENTAL RESULTS

The search for reliable methods of measurement is outlined in Appendix A. The permittivity measurements were made on bars 0.5X0.5X2.5 in. long. A pair of sides was electroded and the specimens were poled.
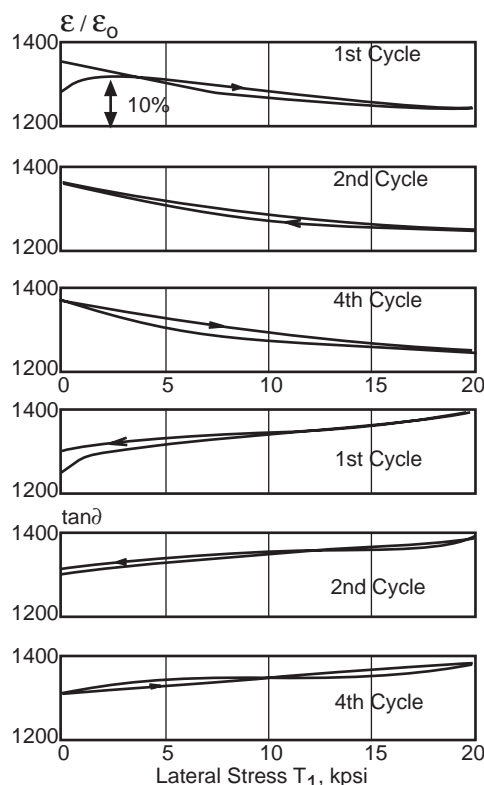

Fig. 1 $\varepsilon / \varepsilon_O$ and tan∂ vs lateral stress (perpendicular to poling axis), T_1; 1st, 2nd & 4th stress cycles. PZT-4

After measurement of capacitance, about 1/2 in. of electrode, length was removed in the center of the bar. With stress along the length of the bar, the two halves were driven out of phase (to avoid driving the press) by a 1-kHz signal at low level. Measurements were normalized to the permittivity obtained before splitting of the electrodes. As for the measurements made for Part 1, detail runs were made for the first, second, and fourth stress cycles. For PZT4 and PZT-8, these were made to a peak stress of 20 kpsi; for PZT-5A to 10 kpsi, and for PZT-5H to 5 kpsi. Specimens were then cycled between zero and peak stress, with measurements made at end points each fifth cycle, for a total of 50 stress cycles The cycling procedure without the detail runs was also carried out at 5, 10, 15, and 20 kpsi, except for PZT-5H, which was subjected to a cycling run at 2.5 kpsi and none at 15 kpsi.
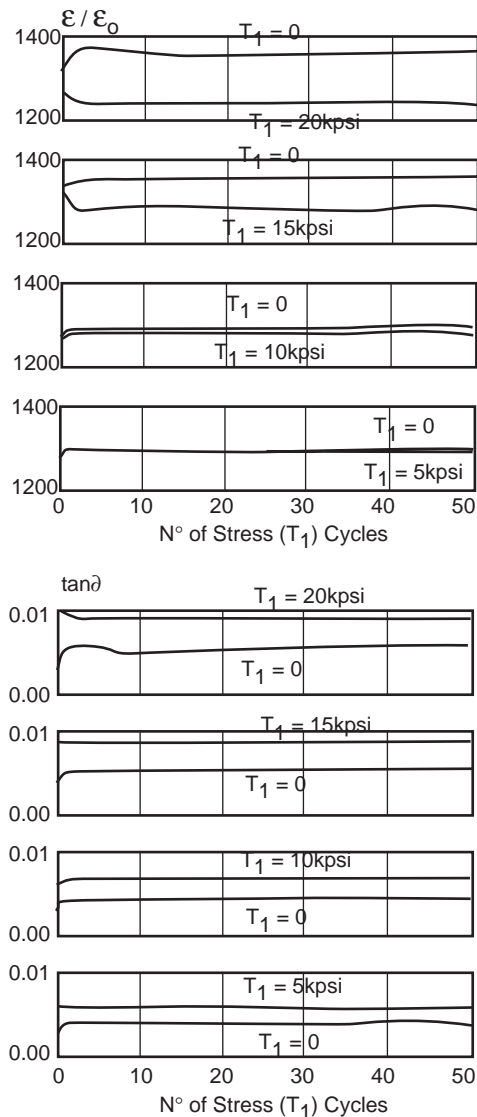

Fig. 2 $\varepsilon / \varepsilon_o$ and tan∂ vs N° of lateral stress cycles to peak stresses of 5, 10, 15 and 20kpsi. PZT-4

Values of d_{31}, and d_{32} were measured using the strain gauge bridge described in the Appendix to Part 1. The same size bars, fully electroded, were used. A large O-ring -compliance was placed in series mechanically to prevent dynamic clamping by the press. Lateral clamping; by the press anvils is minimized by the high lengthto-thickness ratio.

A. PZT-4

Changes in permittivity for PZT-4 are much smaller with lateral static stress (Figs. 1 and 2) than with parallel static stress (Part 1). For the first stress cycle to a peak stress of 20 kpsi, the permittivity shows an initial rise of 2.5% at 4 kpsi, then fail with further increase in stress so that at -20 kpsi the total change as compared to the initial value is -4%. Because the curve does not retrace itself as the stress is reduced below 4 kpsi, the net change after stress removal is +5%. For succeeding cycles, the initial rise is absent, and the values with decreasing stress remain close to those with rising stress. For the fourth cycle, the total change is - 9.5%. After 50 cycles (Fig. 2), the change is still very close to this figure. At lower stresses (Fig. 2), the changes are even less, and for 5 and 10 kpsi are negligible for normal use. The change in tan& is not negligible, but tan∂ remains below 1% for all cases at this low driving-signal level. For high electric drive, the changes shown (Fig. 2, bottom) raise the tan∂-vs electric-field curves in the lie same way as for specimens of higher initial tan∂ (see Appendix to Part 1).
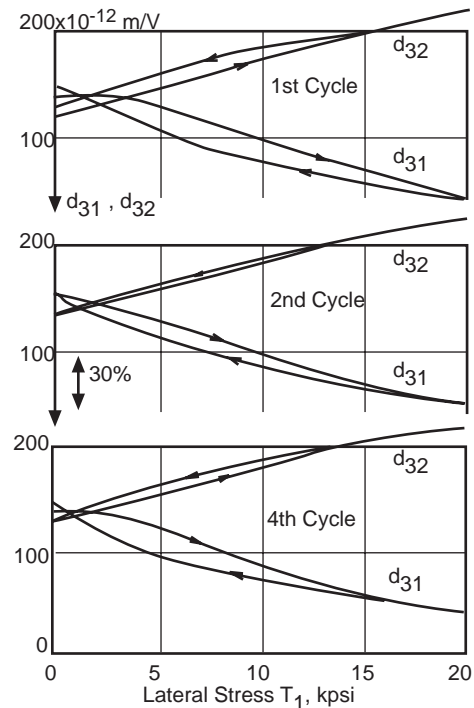

Fig. 3. d_{31}, and d_{32} vs lateral stress, T_1; first, second, and fourth stress cycles. PZT-4

Figures 3 and 4 show the changes of d_{31} and d_{32}, with lateral static stress (T_1). Because of the effective ceramic crystal symmetry (∞ m), the initial values of d_{31} and d_{32} are equal. The mismatch shown in Fig. 3 for PZT-4 is the worst for this series of measurements (a 14% discrepancy) indicating the degree of consistency of the strain-gauge technique. The curves of Fig. 3 show the same character as those of earlier measurements with a large drop (70%) in the d_{31} and a large increase (83%) in d_{32} A small amount of stress stabilization (Fig. 4) reduces the change for 13. to +66% after 10 cycles and to +58% after 30 cycles without fleeting the change in d_{31}. After the first few

2

cycles, he drop in d_{31} is 56% at 15 kpsi, 35%, at 10 kpsi, and 20% at .1 kpsi. Likewise, the rise in d_{32} is 59%, 48%, and 42% for the respective stress-cycle runs.

B. PZT-8

Comparison of Figs. 5-8 for PZT-8 with the respective figures for PZT4 shows that the major point of superiority of PZT-8 over PZT-4 is its lower tan∂, 0.005 or below for all experiments. The change in $\varepsilon^T_{33}/\varepsilon_o$ is slightly greater than for PZT-4 but still very small – -5.5% for the first stress cycle to 20 kpsi, - 9.7% for the fourth cycle, and —9.3% after 50 cycles to 20 kpsi (Fig. 6). The latter figure is the same as for PZT-4
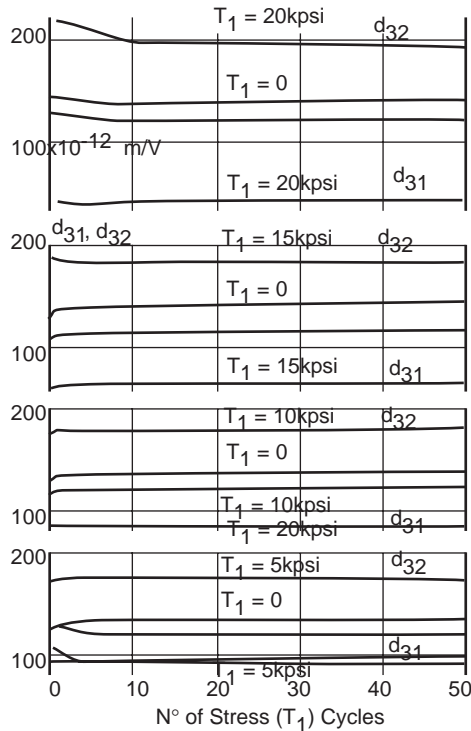

Fig. 4. d_{31} and d_{32} vs number of lateral stress cycles to peak stresses of 5, 10, 15, and 20 kpsi. PZT4.

The cycling runs at 15, 10, and 5 kpsi resulted in permittivity changes of ≈-6%, ≈-4%, and ≈-2%, respectively. Note the anomalously low permittivity of the specimens used for the 10- and 5-kpsi runs. From past experience, this would result in smaller changes of permittivity with environmental changes. This should not invalidate these results, since the changes are negligible for practical purposes. They are, however, larger than for PZT-4.

The changes in d_{31} and d_{32} with static stress T_1 and stress cycling are shown in Figs. 7 and 8. For the first stress cycle to 20 kpsi, d_{31} drops from 93 to 41 X 10-12 m/V, a change of -56%. The fourth and 50th cycles are. the sarne' ≈ - 57%. This compares to a change in dam for PZT-4 of - 70% to this stress. Likewise, the rise in d_{32} is 59% for the first stress cycle and a fairly stable +51% for further cycling, as compared to the slowly

changing curve for PZT4 (+58% after 50 stress cycles). This modest improvement in behavior of PZT-8 over PZT4 is probably the result of its higher mechanical coercive force. Changes are still appreciable for peak stress of 15 kpsi (-45% for d_{31}, +38% for d_{32}), but reasonably small for 10 kpsi (-19% for d_{31}, +20% for d_{32}) and 5 kpsi (-17 and +16170, respectively). At the latter two stress levels, PZT-8 is clearly superior to PZT4.

C. PZT-5A

PZT-5A and PZT-5H are representative of donordoped ceramics that quickly accommodate to stresses.
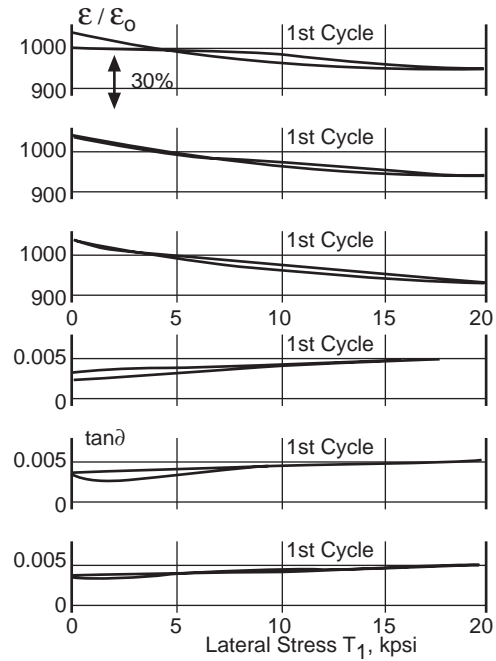

Fig. 5. $\varepsilon^T_{33}/\varepsilon_o$ and tan∂ vs IaLeral stress, T_1; first, second, and fourth stress cycles. PZT-8

Therefore, the first lateral stress cycle for PZT-5A shows the largest change in permittivity (Fig. 9); subsequent Stress cycles are nearly the same as the second cycle. The permittivity of PZT-5A at 10 kpsi is below its initial value by 9.7% for the first stress cycle. By the fourth cycle, the decrease is 6.3% and remains 6.3% to 50 cycles, although the level of $\varepsilon^T_{33}/\varepsilon_o$ has decreased (at zero static stress) by 2.5% from the fourth cycle to the 50th (Fig. 10). For peak stress of 20 kpsi, the drop in permittivity is 7.4% for the fourth cycle, 7.6% for the 50th, while the zero-stress level of permittivity drops by 2%. This behavior is in contrast to that of PZT4 or PZT-8 (Fig. 2 and Fig. 6), for which the level of permittivity after release of stress remains constant after the first few cycles. The level of tan∂ remains high (between 0.013 and 0.020); this and the drastic increase of tan∂ at high ac driving fields shown in Part 1 again relegate the donor-doped ceramics to low power or hydrophone uses.
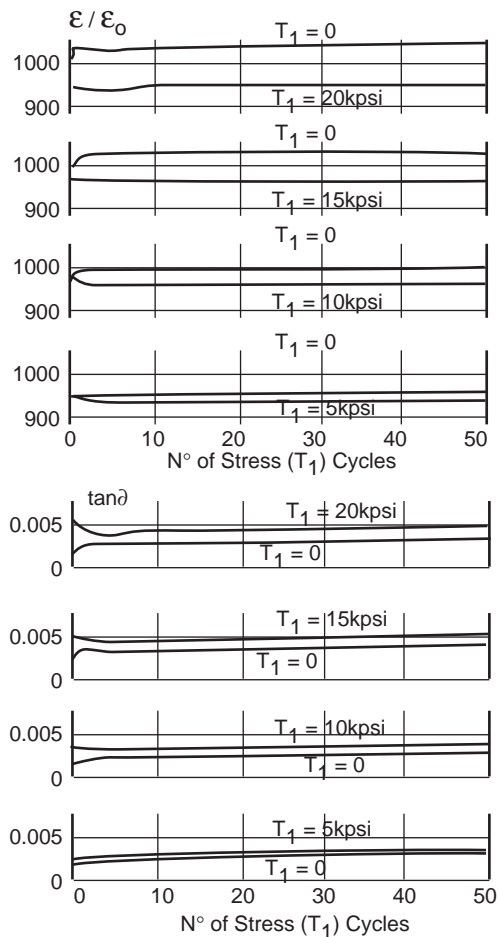
3

FIG. 6. $\varepsilon^{T}_{33}/\varepsilon_{o}$ and tan∂ vs number of lateral stress cycles to peak stresses of 5, 10, 15, and 20 kpsi PZT-8
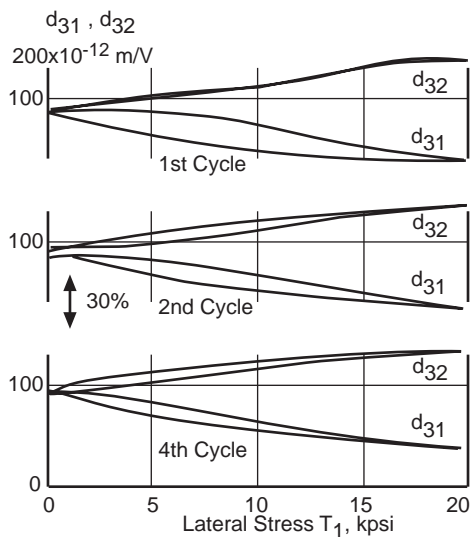

Fig. 7. d_{31} and d_{32} vs lateral stress, T_1 first, second, and fourth Aress cycles PZT-8

The changes of d_{31} and d_{32} with static lateral compressive stress T_I are shown in Figs. 11 and 12. An effect which is barely hinted at in the corresponding curves for the "hard" ceramics is demonstrated outstandingly by these curves for PZT-5A and Figs. 15 and 16 for PZT-5H. Not only do d_{31} and d_{32} separate under stress (Figs. 11 and 15), but the recovery on release of stress is never perfect (very poor for 15 and

20 kpsi, Figs. 12 and 16), resulting in permanently different d_{31} and d_{32} The stress changes the ceramic
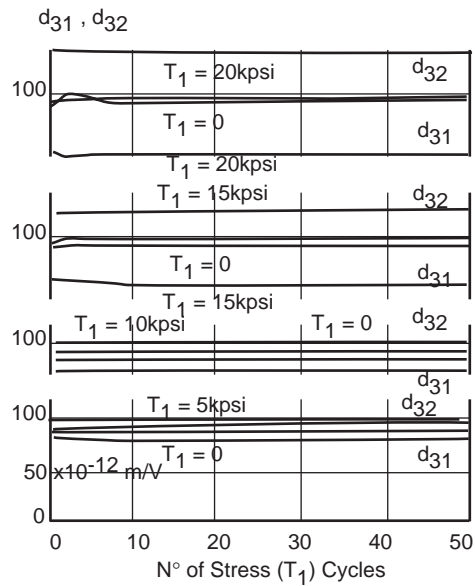

Fig. 8. d_{31} and d_{32} vs number of lateral stress cycles; to peak stresses of 5, 10, 15, and 20 kpsi. PZT-8.

symmetry from coin (isotropic in the plane perpendicular to the polar axis) to 2mm or to a pseudo-orthorhombic symmetry. This effect was noted previously' but not shown as clearly as in this detailed study. The 20-k-psi cycling run (Fig. 12), for instance,
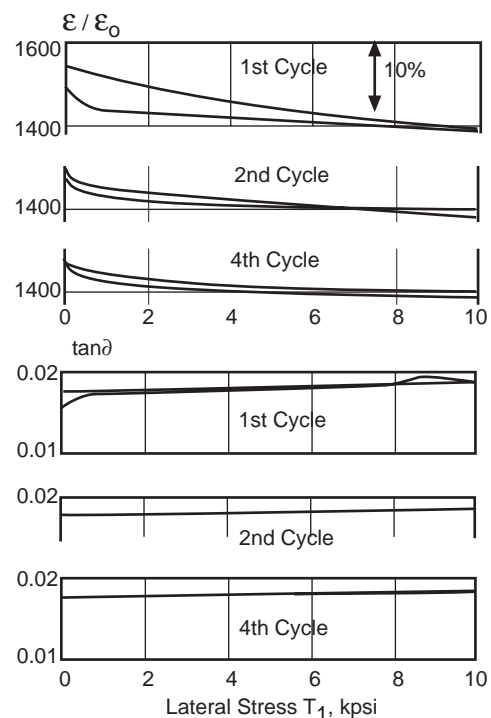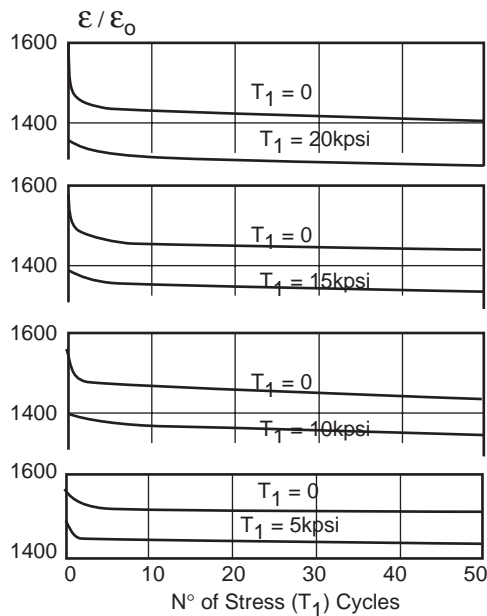

FIG. 9. $\varepsilon^{T}_{33}/\varepsilon_{o}$ and tan∂ vs lateral stress, Ti; first, second and fourth stress cycles. PZT-5A

shows a 2: 1 ratio of d_{33} to d_{31} after a few lateral stress cycles. It is possible through static-bias stress in a chosen 1-direction to increase response to dynamic skew in the direction perpendicular to this and the polar axis. With PZT-5A or PZT-5H, some improveFir..

4

10. $\varepsilon^T_{33}/\varepsilon_o$ vs number of lateral stress cycles to peak stresses of 5, 10, 15, and 20 kpsi PZT-5A

FIG. 11. d_{31} and d_{32} vs lateral stress, T_1 ; first, second,
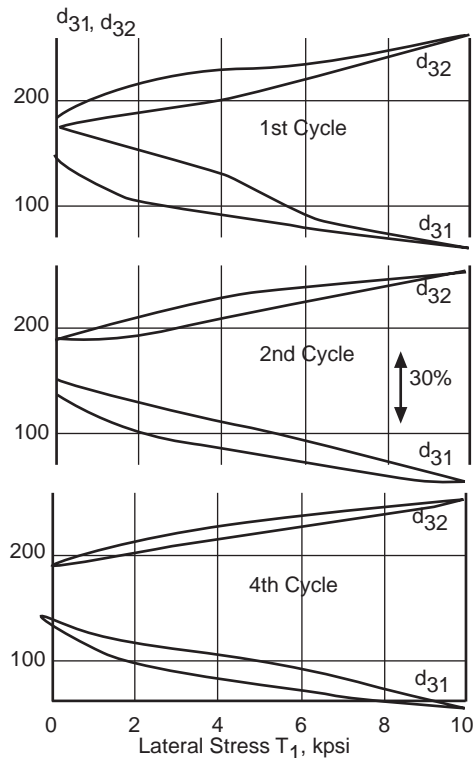

Fig. 12. d_{31} and d_{33} vs number of lateral stress cycles to peak stresses of 5, 10, 15, and 20 kpsi. PZT-5A

and fourth stress cycles, PZT-5A

Fic. 13. $\varepsilon^T_{33}/\varepsilon_o$ and $\tan\partial$ vs lateral stress, T_1; second, and fourth stress cycles. PZT-5H.

ment is possible on a remanent basis- i.e., the stress need not remain applied. This is easy to do with a radially poled tube by stressing with a bolt through its center and then making use of the response to circumferential stress. The improvement possible for PZT-5A would be ~20% with a remanent effect and 65% for a maintained bias stress of 20 or 15 kpsi. For hydrophone design of the usual sort, the stress applied by depth will be in the direction of the useful response, decreasing that response as shown in the curves. Useful response for PZT-5A (d_{31}~100X10^{-12} m/ V) is still available at 5 kpsi. PZT4 would perform relatively better at higher stresses.
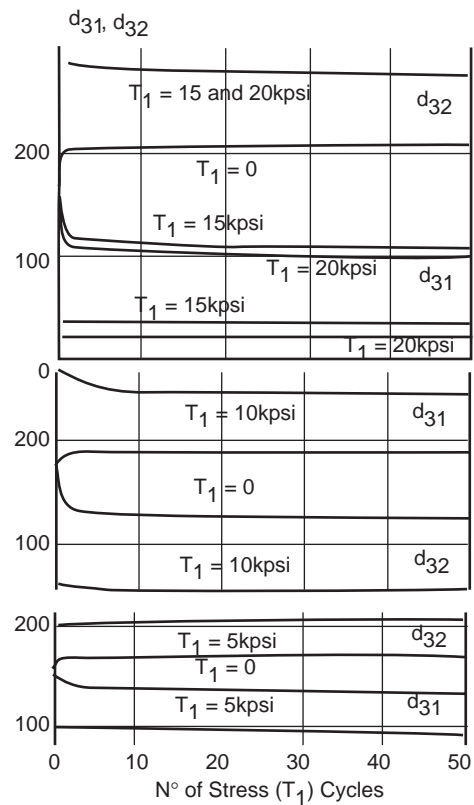
D. PZT-5H

PZT-5H has high values of d_{31} and d_{33} and permittivity, making it useful for hydrophones, where low impedance and high output are desirable. With its d_{31} (standard value - 274x10^{-12} m/V) comparable to the d33 of PZT-4 (standard value 289x10^{-12} m/V), the (often) simpler transducer geometries using lateral response can be used effectively. The effects of static lateral stress (T$_1$) on $\mathcal{E}^T_{33}/\mathcal{E}_o$ d_{31} and d_{32} are shown in Figs. 13-16. Permittivity changes are somewhat greater than for the other ceramics (- 14%) at 20 kpsi, - 9% at 10 kpsi, -9% at 5 kpsi, and even -6.5% at
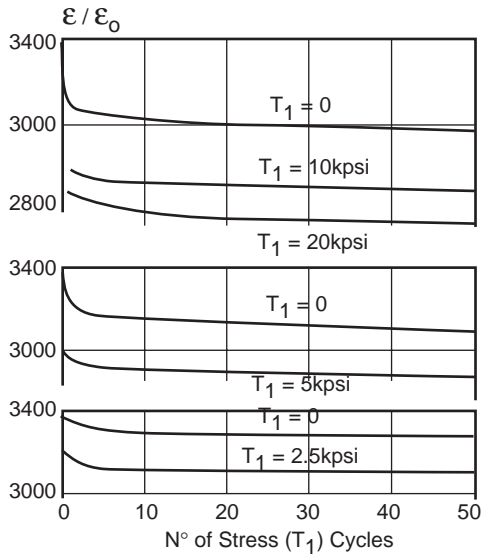
FIG. 14. $\mathcal{E}^T_{33}/\mathcal{E}_o$ vs number of lateral stress cycles to peak stresses of 2.5, 5, 10, and 20 kpsi PZT-5H

2.5 kpsi); but these are still unimportant changes, particularly in view of the recommended use of PZT-5H in receivers only. Figure 15 shows d_{31} and d_{32} for stress runs to 5 kpsi. Percentage changes are seen to be comparable to the hard ceramics for stress runs to 20 kpsi, and recovery is very poor, giving even greater disparity between d_{31} and d_{32} than for comparable stress in PZT-5A

IL **DISCUSSION**

Where the need is for radiated power and efficiency, the relatively good behaviour under conditions of high electric field of the "hard" ceramics PZT-4 and PZT-8) eliminates consideration of the "soft" ceramics. For hydrophone service, the choice is not so clear. Figure 17 summarizes the results of the effects of lateral stress (T$_1$) on dal and d_{32} for the four ceramic materials studied here. The points are derived from the stresscycle curves, using the data for the 10th cycle, and normalized to the published nominal values of d_{31} Similar "cross plots could be made for the first and 50th stress cycles; but major changes have occurred by the 10th cycle, making it a good compromise for such a plot. The ceramic of highest charge sensitivity (d_{31}) depends on tile operational stress. At 3800 psi, d_{31} for PZT-5H crosses that for PZT-5A at 6500 psi, d_{31} for PZT-5A crosses that for PZT4; and at
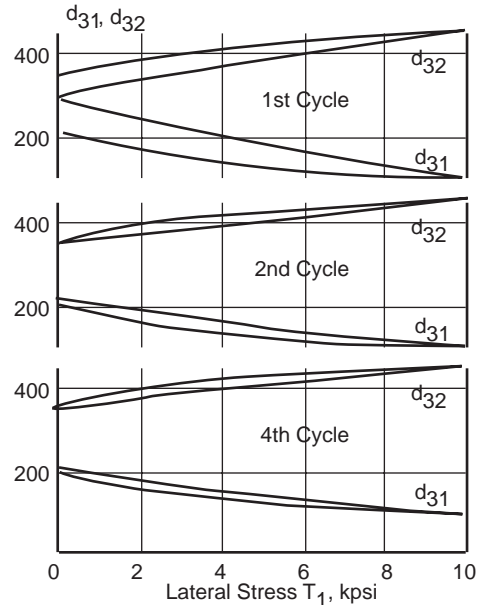
Fig. 15. d_{31} and d_{32} vs lateral stress, T$_1$ first, second and fourth stress cycles. PZT-5H.
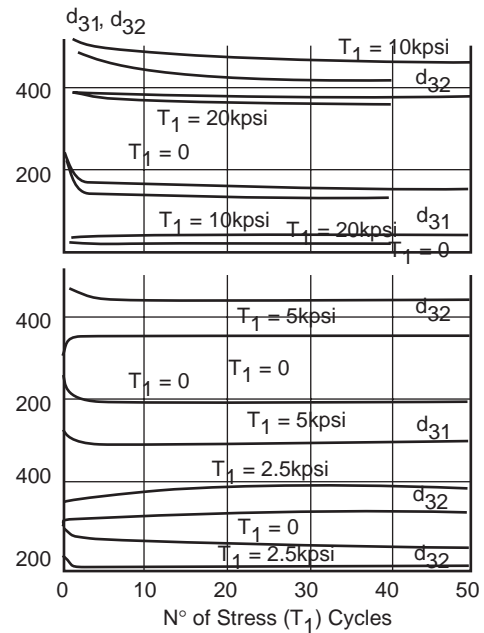
Fig. 16. d_{31} and d_{32} vs number of lateral stress cycles to peak stream of 2.5, 5, 10. and 20 kpsi. PZT-5H

7200 that for PZT-8. For relatively constant response for bias stress to 10 kpsi, PZT-8 is superior, in spite of its low level of response.

Figure 17 also shows that, if a prestress design can be used, large improvements in response can be realized by using the response to dynamic stress perpendicular to the bias stress and polar axis (d_{32}) This does not mean that PZT-511 could be prestressed to 10 kpsi and then submerged to 5 or 10 kpsi and still give the d_{32}=435x 10^{-12} m/V sensitivity indicated in Fig. 17. Brown' has shown that two-dimensional or planar stress results in drastic changes in the permittivity. of certain ceramics, including PZT-4 changes that also affect the d constants. One must hedge further on

designs based on large prestress, for little is known about mechanical creep acting to relieve the stress or about the aging of the enhanced d_{32} and of the permittivity under these conditions of stress. Nevertheless, large improvements in laterally stressed transducers should be possible for shallow-depth hy drophones, and at least one such attempt has been made (successfully), using PZT-4 Hydrophones based on enhanced remanent d_{32} where the enhancing stress has been removed, or other uses of the pseudo-orthorombic ceramic that results after release of large lateral stresses applied to the donor-doped ceramics have not come to the author's attention.
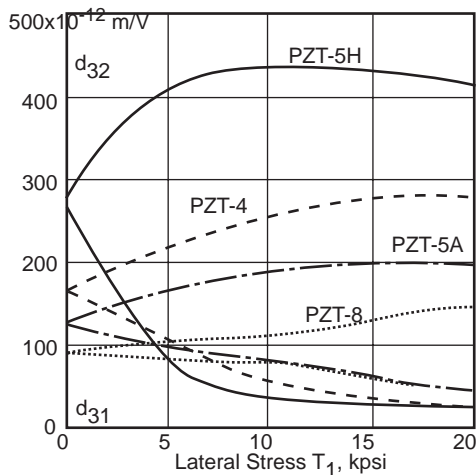

Fig. 17. d_{31} and d_{32} vs lateral stress, T_1 Comparison of all ceramics tested. Data taken from end points of the 10th stress cycle (Figs. 4, 8, 12, acid 16) normalized to published nominal values of d_{31} and d_{32}

Apart from design considerations, the concurrent rise of d_{32} and fall of list for stress T, (reversible for the "hard" ceramics) pose an interesting theoretical prob. lem. A poled ceramic has the majority (but not all) of domains aligned in the closest of the allowed crystallographic directions to the poling electric-field vector. Reversible domain-wall motion enhances permittivity and piezoelectric constants, and this is due primarily to unaligned domains. With tetragonal perovskites, as those in this study, the reversible domain-wall motion is primarily due to 90° switching. It should be noted that stress will generally promote 90' switching, and an electric field will promote both 90° and 180° switching. Permittivity is much lower along the polar axis of a crystallite than in the perpendicular plane. Thus, compressive stress along the polar axis tends to increase permittivity drastically because anisotropy of the permittivitv and creation of additional domain walls act together. Compressive stress perpendicular to the polar axis tends to create relatively few additional domain walls in a poled material and furthermore does not drastically affect domain alignment. The effect on the permittivity is therefore fairly small. However, taking 1 as the direction of the static stress, it can be seen that some crystallites, oriented during poling so that the cube edge of the unit cell nearest the, electric-field vector (3) is polar, actually have another cube edge closer to the

plane perpendicular to 1. Domains in these crystallites tend to switch during lateral compression. In addition, some domains that were not oriented by the poling process become , aligned by lateral compression. This alignment is not polar (180" twinning), however. This creates a situation such that there is little

contribution to response to dynamic-stress along -1 by reversible domain wall movement, therefore reducing d_{31} Domains oriented in the plane perpendicular to I nearly parallel to 2 arc those that are particularly unstable, since they were mostly switched to nearly parallel to 3 by the static stress. Reversible contributions of these domains with dynamic stress along 2 enhance d_{32} markedly.
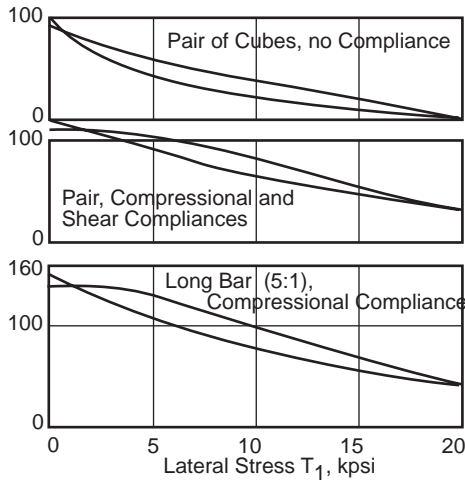
ACKNOWLEDGMENTS

Appendix A

Problems associated with measurement of properties with static strew parallel to the poling axis (T_3) are discussed in the Appendix to Part 1. The experimental method that worked best consisted of using a pair of specimens driven out of phase. Primarily, this avoided driving the mechanical press, and therefore press resonances (which invariably showed up as loss peaks during permittivity measurements made without this precaution) were not excited.. Perhaps equally important, this method ensured dynamically free conditions for the permittivity measurements. In spite of rather large bias stresses, the incremental strains necessary for the measurements were not blocked or clamped, except for some lateral clamping at the press anvils and at the specimenspecimen interface. Because $d_{31} \approx -0.45 \, d_{32}$ a cube was deemed sufficiently long to consider the specimens laterally free. The same technique was tried initially for measurements of properties under lateral stress (T_1) and found unsatisfactory. Apparently, the clamping lateral to the stress is large when the piezoelectric motion is large; i.e., the motion along the poling direction is clamped, reducing the measured value of d_{31}. Two methods were found successful for relieving this clamping: the first involved rubber shims between specimens and anvils. The low shear modulus of the rubber then allowed the lateral motions. The second required use of a bar of length to width/thickness of 5:1. With a bar this long, the clamping of the ends had little effect at the center of the bar, where the strain gauges were mounted for

7

measurement of d_{31} and d_{32} The latter was the technique chosen for measurement

FigA-1, d_{31} vs lateral strut T1 as measured under various experimental configurations for PZT-4.

Fig. A-2. $\varepsilon^T_{33}/\varepsilon_o$ and tan∂ vs lateral stress T_1 as measured under various experimental configurations for PZT-5H

of d constants because the alignment of the specimen in the press was easier than with the first method and specimen breakage was reduced.' Apparently, the rubber's folding itself around the sharp corners of the ceramic increased the stress on the corners sufficiently to produce a stress gradient that sheared columnar chips off the specimens. (It has always been our experience, that hard, well-finished, anvils broke fewer specimens than any kind of soft anvil or soft spacer.) A large O-ring between fiber spacers provided the compliance in the stress direction to allow free piezoelectric motions. Figure A-1 shows typical results for PZT-4 with the various measurement techniques. Early measurements with single cubes and a relatively stiff Bakelite compliance showed large low stress increases in d_{31} that could only be explained by assuming that a broad, low-Q resonance was excited in the press. The upper curve of Fig. A-1 shows low initial d_{31}. This occurred for cubes with nominal d_{33} and d_{31} after the pair was assembled for out-of-phase drive, and, before installation in the press, apparently due to clamping at the specimen-specimen interface.

Several measurements of permittivity were made using the "long-bar" technique; but again peaks in tan∂ showed up, indicating that the press was being driven in spite of the series compliance. This was avoided by. splitting the electrodes on the long bar and driving the two halves out of phase. This sacrifices effective length and introduces another uncertainty at the electrode gap, where the field is such as to excite two opposing shear deformations. Nevertheless, because of its simplicity in alignment and the good behaviour of the tan∂ during measurement, this technique was accepted as standard. Figure A-2 shows measurements made on PZT-5H with a 5:1 fully electroded bar and a 5: 1 split-electrode bar. Note the smooth progression of points for the curve for which the drive was out of phase compared to the peaks in tan∂, particularly, for the fully electroded long bar, where driving of the press cannot be avoided. Measurements of permittivity on pairs of cubes were also made. Again, lateral clamping significantly. reduced the permittivity, though the outof-phase drive resulted in tan∂ behaviour the same as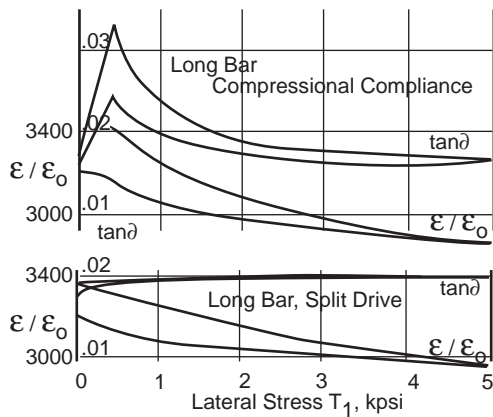 shown in the lower curve of Fig. A-2.